1-1-2005

Power Enhancement of an Actively Controlled Battery/ Ultracapacitor Hybrid

Lijun Gao
Boeing, Lijun.gao@boeing.com

Roger A. Dougal
University of South Carolina - Columbia, dougal@engr.sc.edu

Shengyi Liu
Boeing, shengyi.liu@boeing.com

Publication Info

Published in *IEEE Transactions on Power Electronics*, Volume 20, 2005, pages 236-243.

Power Enhancement of an Actively Controlled Battery/Ultracapacitor Hybrid

Lijun Gao, *Member, IEEE*, Roger A. Dougal, *Senior Member, IEEE*, and Shengyi Liu, *Senior Member, IEEE*

***Abstract*—An actively controlled battery/ultracapacitor hybrid has broad applications in pulse-operated power systems. A converter is used to actively control the power flow from a battery, to couple the battery to an ultracapacitor for power enhancement, and to deliver the power to a load efficiently. The experimental and simulation results show that the hybrid can achieve much greater specific power while reducing battery current and its internal loss. A specific example of the hybrid built from two size 18650 lithium-ion cells and two 100-F ultracapacitors achieved a peak power of 132 W which is a three-times improvement in peak power compared to the passive hybrid power source (hybrid without a converter), and a seven times improvement as compared to the lithium-ion cells alone. The design presented here can be scaled to larger or smaller power capacities for a variety of applications.**

***Index Terms*—Hybrid power source, lithium-ion battery, peak power enhancement, power converter, ultracapacitor.**

I. Introduction

MANY classes of power systems, such as those in portable electronic devices, telecommunication systems, spacecraft power systems, and electric vehicles, have a common characteristic in their load profiles. That is, they have a relatively low average power requirement but a relatively high pulse power requirement. The typical pulse duration in these applications generally ranges from hundreds of milliseconds to seconds, with power levels depending on the applications. Battery/ultracapacitor hybrid power sources can meet these pulse power requirements with higher specific power and efficiency than batteries alone.

An ultracapacitor, also referred to as a supercapacitor or an electrochemical double layer capacitor [1], [2], stores charge in a double layer formed on a large surface area of micro-porous material such as activated carbon. Generally, such devices have specific energy in the range of 1 to 10 Wh/kg and high specific power in the range of 1000 to 5000 W/kg. The charge/discharge efficiency of ultracapacitors is very high, ranging from 85% to 98%, and the rate of discharge can be fast, ranging from 0.3 to 30 s. The lithium-ion rechargeable battery, in contrast, has a higher specific energy in the range of 50 to 500 Wh/kg and a lower specific power between 10 and 500 W/kg. Its charge/discharge efficiency is in the range of 75% to 90%, and the rate of discharge is typically between 0.3 and 3 h. A combination of battery and ultracapacitor can take advantage of each kind of device to yield a power source of both high power density and high energy density.

Research on hybrid power sources [3]–[7] demonstrates that the combination of ultracapacitors and batteries achieves a longer run-time and a higher power capability compared to a battery-alone under a pulsed load condition. A major characteristic of the hybrid power sources described in these prior studies is the direct connection of the battery and ultracapacitor in parallel, as shown in Fig. 1; therefore, the power sharing between the battery and the ultracapacitor is determined by their respective resistances. The terminal voltage of such a hybrid power source is not regulated but instead follows the battery discharge curve and can vary considerably between fully charged and fully depleted. In this paper, we describe an improved battery/ultracapacitor hybrid that incorporates a dc/dc converter between the two energy storage elements, as shown in Fig. 2. The converter is used to actively control the power flow from the battery to the ultracapacitor and the load, thereby enhancing the power capability. The study results show that, for a current load pulsing at a rate of 0.2 Hz at a 10% duty ratio, the power capability of an actively controlled hybrid can be nearly three times greater than that of a passive hybrid having the same battery and ultracapacitor sizes. In addition, the active hybrid offers advantages of a broader output voltage range, better output voltage regulation, a smaller battery current ripple, and less weight and volume of the system.

The actively controlled hybrid was studied via both simulations and experiments. The simulation studies are conducted in the virtual test bed (VTB) [8]–[10] environment with prevalidated dynamic models of a lithium-ion battery and an ultracapacitor. For specific results, we used the Sony US18650 lithium-ion batteries and Maxwell PC100 ultracapacitors since we had good characterizations and models of those particular items. Models of each have been described in [11] and [12], respectively.

In the section that follows, we will first discuss the advantages of active hybrids over passive ones. Then in Section III, the details of the actively controlled hybrid—simulation study, converter and controller design, experimental implementation, simulation and experiment results—are presented. Section IV discusses the performances of the active hybrid power source in comparison to the passive one for some particular load profiles. Conclusions are drawn in Section V.

II. Actively Controlled Hybrid Power Sources

As has been demonstrated, an optimized passive battery/ultracapacitor hybrid [6] has several advantages over a

Manuscript received September 17, 2003; revised July 13, 2004. This work was supported by NRO under Contract NRO-00-C-1034, by ONR under Contract N00014-00-1-0368, and by ONR under Contract N00014-00-1-0131. Recommended by Associate Editor K. Ngo.

The authors are with the Department of Electrical Engineering, University of South Carolina, Columbia, SC 29208 USA (e-mail: gaolijun@engr.sc.edu).

Digital Object Identifier 10.1109/TPEL.2004.839784

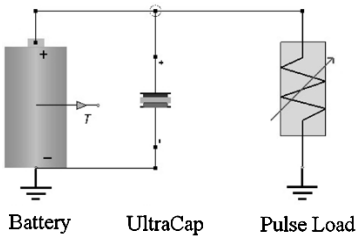

Fig. 1. VTB schematic of passive hybrid.

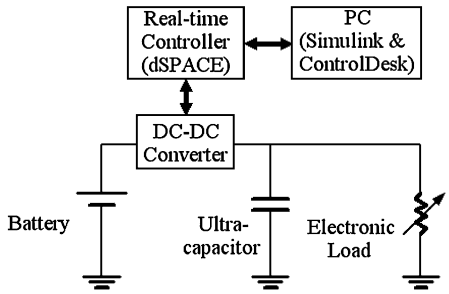

Fig. 2. Actively controlled battery/ultracapacitor hybrid.

battery-alone power source, such as higher peak power capability, higher efficiency, and longer battery cycle life. However, the fact that the battery and ultracapacitor are directly connected limits the performance of this hybrid architecture. First of all, the ultracapacitor terminal voltage and the load voltage both float with the battery terminal voltage (depending on state of charge), which prevents the power capability of the ultracapacitor from being fully exploited. For the same reason, the choice of the ultracapacitor array size is restricted by the terminal voltage of the battery since the upper limit of the ultracapacitor voltage generally cannot be an arbitrary value. Secondly, the power enhancement of the passive hybrid source is limited by the partitioning of current between the battery and the ultracapacitor, which is predominantly determined by the equivalent series resistances of the two components. The battery current may have a large ripple during the pulse on-time and the ripple reaches a maximum value at the end of the current pulse, which may result in shutting off any built-in battery protection circuit (common in lithium-ion batteries). Finally, the terminal voltage of the passive hybrid is not regulated, but instead follows the discharge curve of the battery and can vary considerably between fully charged and fully depleted. For example, the terminal voltage of four lithium-ion cells in series may drop 6.8 volts from fully charged to fully depleted (16.8 to 10 V), equal to a voltage variation of 68% relative to the final voltage.

Adding a dc/dc converter between the battery and the ultracapacitor yields several advantages: 1) the ultracapacitor voltage can be different from the battery voltage, which offers flexibility with respect to the design of the battery and ultracapacitor arrays, 2) the power capacity can be much higher than that of the passive hybrid without exceeding the safety limit of the battery current, 3) the power source terminal voltage can be kept relatively constant, with a smaller variation than that of the passive source even as the battery is depleted, 4) the weight of the power source for a given peak power can be smaller than that of a passive power source for the same load, and 5) the dc/dc converter

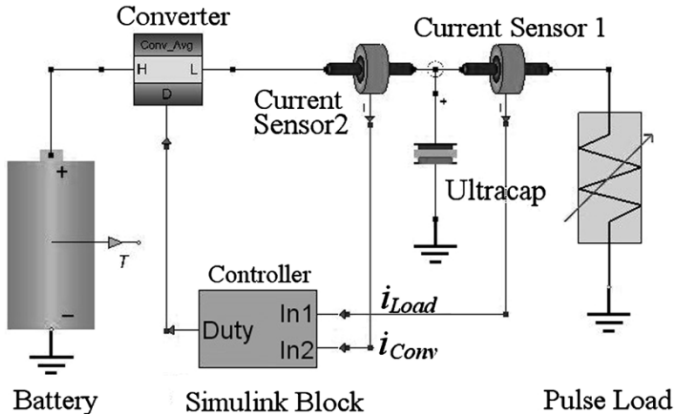

Fig. 3. Virtual prototype of the active hybrid.

can also serve as the battery charging regulator while a passive hybrid power source would require a separate battery charger.

The principle of operation of such an actively controlled hybrid is described as follows: When the load current is small, the converter is controlled such that the battery discharges at a constant rate regardless of the battery voltage variation, and it charges the ultracapacitor. The discharge rate of the battery is determined by the average load demand, and is controlled via an appropriate feedback mechanism. To protect the battery, the current is controlled so as to not exceed the safety limit. At this time, the ultracapacitor is charged at a constant current, but the level of the current is higher than the battery current (if the converter is step-down) and determined by the duty ratio of the converter. Secondly, when the load current is high, both the battery and the ultracapacitor supply current to the load. However, the battery current is still controlled at the same constant rate so that the rest of the current, at a much higher level, will be supplied by the ultracapacitor. By controlling the battery current at a constant value throughout the operating cycle, the battery is in an extremely steady state, it is therefore electrically and thermally preferred for the sake of a safe and long lifetime. Most importantly, the hybrid provides much higher power without drawing excessive current from the battery.

III. Simulation and Experiment

A. Virtual Prototyping

A virtual prototype of the active hybrid system, as described by Fig. 2, was first built in the VTB to prove the concept and verify the design. The system schematic in VTB is illustrated in Fig. 3. In the active system, the models of the battery, the ultracapacitor and the load were the same as those used in the passive system, but the configurations were different. The battery (shown as only one icon in the schematic) consisted of two lithium-ion cells connected in series whereas in the passive system the two cells had to be connected in parallel in order to keep the voltage within the operating range of the ultracapacitor. The ultracapacitor consisted of two cells also connected in series. The dc/dc step-down converter model was a time-averaged model. The converter was controlled by a PI (proportional-integral) controller represented by the controller block in the schematic diagram. The controller block is a wrapper object that allows the VTB to interactively co-simulate with

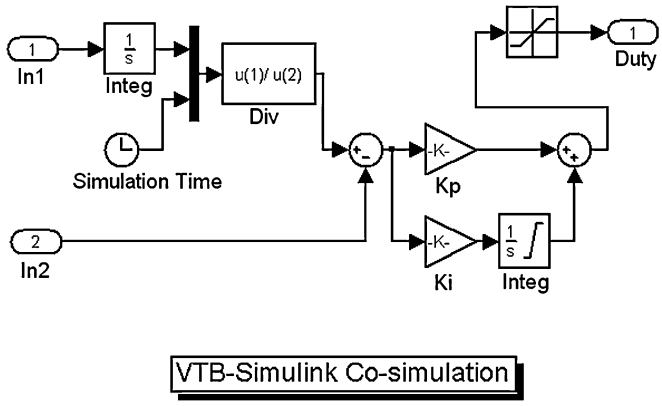

Fig. 4. Control algorithm implemented in the Matlab/Simulink.

the controller that is defined in the Matlab/Simulink. The controller block had two input ports (In1 and In2) that were connected to two current sensors that monitored the load current and the power converter output current, respectively. The monitored current signals were then fed to the PI controller; and the new calculated converter duty ratio from the PI controller was sent back to the power converter model in the VTB through the output port (Duty).

The Simulink implementation of the PI controller is shown in Fig. 4. The two input ports (In1 and In2) received the measured current signals and the output port (Duty) sent the new calculated duty ratio to the power converter. The controller's goal was to keep the output current of the power converter at a relatively constant value equal to the load time-averaged current. This buffered the battery from high pulse currents, and maintained a relatively constant ultracapacitor voltage. It can be seen in Fig. 4 that the load current received from input port In1 was first integrated and then was averaged according to the current simulation time. After that, the calculated time-averaged load current was compared to the power converter output current received from input port In2 and the error between them was then fed to the proportion-integrator. While it is obvious that more sophisticated control algorithms could be designed, this simple algorithm is sufficient to demonstrate the essential capabilities of an actively controlled hybrid power source. The test shows that this controller ensured zero steady-state error, and that the output of the hybrid power sources did follow the load demand.

B. Experimental Implementation

After the simulation study, the active hybrid power source was built using real hardware. Fig. 5 shows a photograph of the experimental setup, and Table I lists the parameters of the main components. A dSPACE [13] real time controller controlled the dc/dc converter. Controller code was generated and compiled directly from the Matlab/Simulink and then downloaded to the dSPACE hardware.

The pulse current demand was generated by an electronic load using the same pulse profile that was defined for the simulation experiment. The load was set to the external programming mode with the pulse control signal coming from the dSPACE digital output port. Experimental data was logged at 250 samples/s. Fig. 6 shows the circuit diagram of the synchronous buck converter. A voltage chopper consisting of a main switch Q_1 and

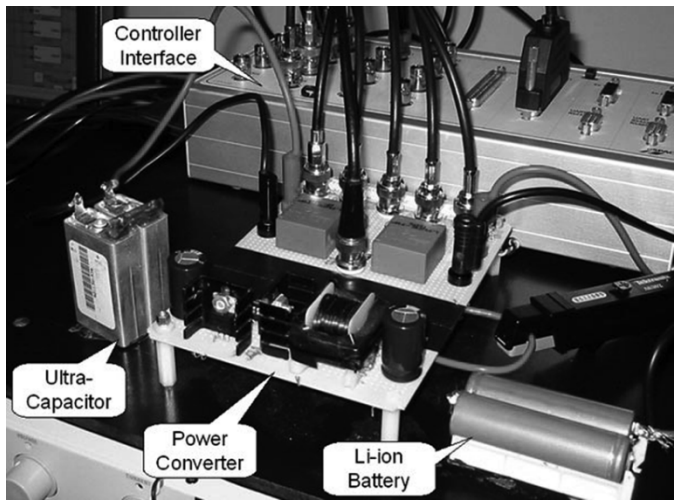

Fig. 5. Experimental setup of the active hybrid system.

TABLE I
SPECIFICATIONS OF THE ACTIVE HYBRID POWER SOURCE

Battery Pack (SonyUS18650)	2 cells in series, total 84 g, 138.4 cm^3 1.4 Ah/cell, I_{MAX} = 2.4A/cell, Nominal 3.8V/cell, V_{Cutoff} = 2.5V
Ultracapacitor (Maxwell PC100)	2 cells in series, total 74 g, 64.0 cm^3, V_{MAX} = 2.7V
Pulse Load (Agilent Tech. 6060B)	0.2 Hz, 10% duty
Controller	dSPACE DS1103 PPC Controller Board
DC/DC Converter	L= 90μH, C= 470 μF, f=50 kHz, efficiency 92.5%

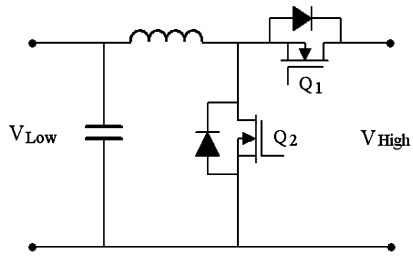

Fig. 6. Circuit of the dc/dc converter.

a secondary switch Q_2 (operating as a synchronous rectifier) converted the voltage from the battery pack to an appropriate lower voltage for the ultracapacitor. The component values of the converter are listed in Table I.

C. Operating Characteristics

The simulation and experimental results for the active hybrid are presented in this section for an example case study of a pulse current discharge of about 30 A, a pulse rate of 0.2 Hz, and a duty ratio of 10%. The current level was chosen so that the battery current was below the safe limit. The load pulse duty ratio affects both the power enhancement and the efficiency for a given configuration of the battery and ultracapacitor arrays [6]. Considering both power enhancement and efficiency, we chose 0.1 as the duty ratio which yielded a pulse duration of 0.5 s. This duration falls within the range that interests us for most pulsed-operations as discussed in the introduction.

The electrical characteristics of the active power source presented here include time-varying behaviors of the current, the voltage, and the power. Fig. 7 shows the simulation results for the current waveforms. The programmable load drew current pulses as specified previously. The converter output current was

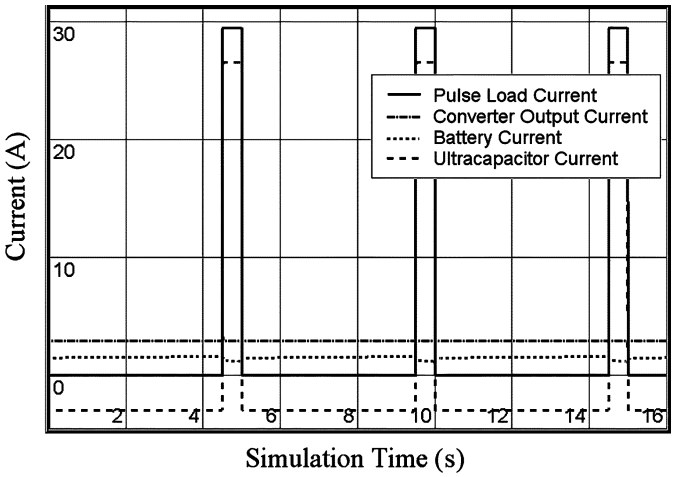

Fig. 7. Simulation results of the current waveforms of the active hybrid.

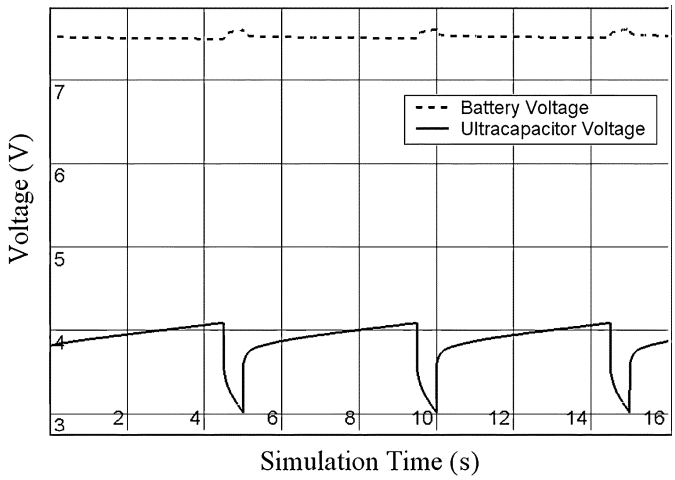

Fig. 8. Simulation results of the voltage waveforms of the active hybrid.

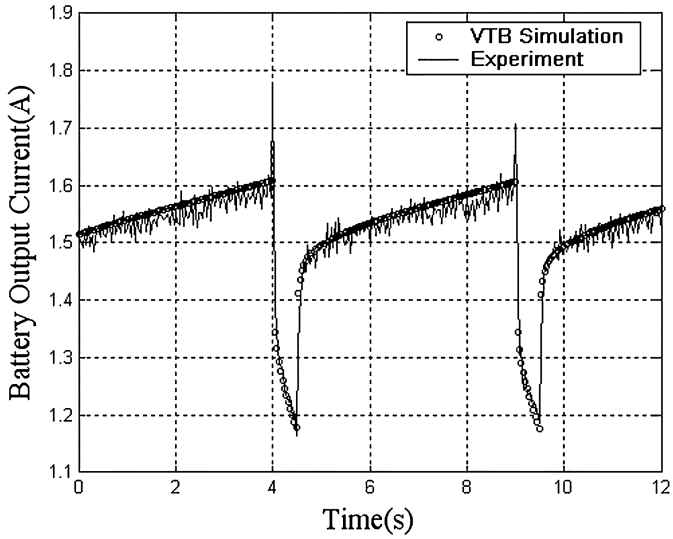

Fig. 9. Comparison of the simulated and experimental battery current.

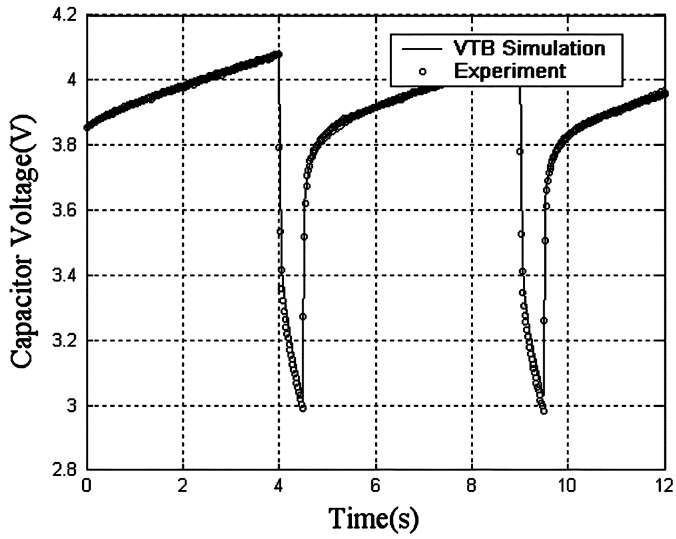

Fig. 10. Comparison of the simulated and experimental ultracapacitor voltage.

constant throughout the entire load cycle (about 2.94 A), and equaled to the average value of the load current. The battery current was also nearly constant except for a small variation of about 0.1 A increase during the pulse-off time and 0.4 A decrease during the pulse-on time, with a ripple amplitude of 0.5 A. The ultracapacitor current was negative (charging) when the load current was zero and positive (discharging) when the load current was high. During the discharging phase, the ultracapacitor supplied 90% (26.46 A) of the load current. Only 10% of the load current was provided by the converter, which converted to a battery current of less than a half of 10% due to a step-down conversion effect, much lower than the battery safety limit. The simulation results for the battery and ultracapacitor voltages are illustrated in Fig. 8. During each pulse-on time, the terminal voltage at the ultracapacitor dropped from approximately 4.1 V to about 3.0 V (about 1.1 V variation) while the battery voltage remained almost constant (about 7.5 V) for the entire period, with a little increase during the high current phase.

The experimental data in comparison to the simulation results are shown in Figs. 9, 10, and 11 for the battery current, ultracapacitor voltage, and converter output power, respectively. Notice that, in Fig. 9, the battery current waveform was zoomed out for a better resolution, showing 0.1 A increase when the load current was zero, and 0.4 A decrease when the load current was high. These variations were consistent with the simulation result as indicated by the circular data points. The measured result confirmed that the battery current in the hybrid power source was nearly constant even for a high pulse current operation. For the ultracapacitor voltage and the converter output power, the experimental and the simulation results were also well-matched, as shown in Figs. 10 and 11, respectively. The ultracapacitor voltage, equal to the load voltage, had about a 1.1 V variation due to the ultracapacitor switching from a charging mode to a discharging mode. The converter output power, equal to the battery output power, had a 3 W variation in each load cycle. The power increased and reached the maximum value of 12 W before the load current pulse started, and then decreased during the high current pulse to the minimum value of 9 W at the end of the pulse. The agreement between the simulation and the experimental results successfully validated both the experimental design of the hybrid system and the simulation models of the system.

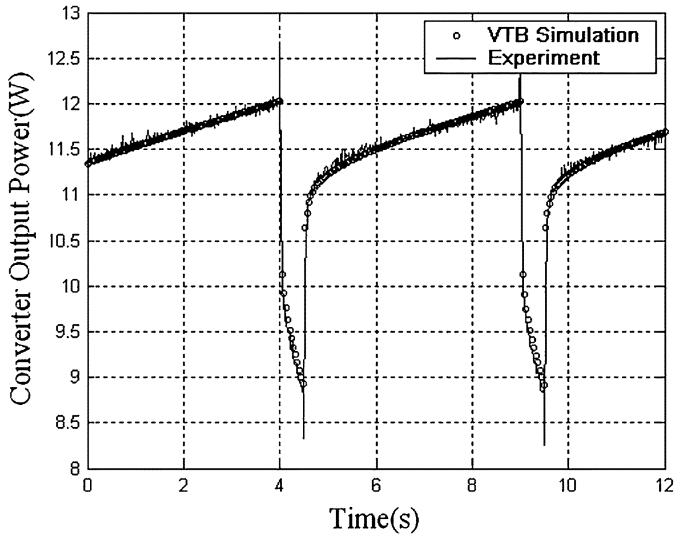

Fig. 11. Comparison of the simulated and experimental converter output power.

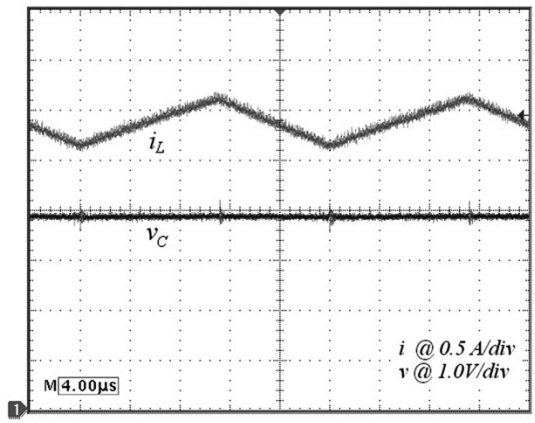

Fig. 12. Inductor current (0.5 A/div) and the converter output voltage (1 V/div) when the load demand is low.

Figs. 12 and 13 illustrate oscillograms of the operating power converter. Fig. 12 shows one switching cycle of the inductor current and converter output voltage when the pulse load demand was low. The switching frequency of the power converter was set at 50 kHz; thus the period of one switching cycle was 20 μs. It can be seen that the inductor current had a ripple of 0.45 A and the average value was about 3 A. The converter output voltage at the measured switching cycle was around 3.95 V. Fig. 13 shows one switching cycle when the load demand was high. The inductor current remained at 3 A with a ripple 0.45 A; however, the converter output voltage during the measured switching cycle was around 3.2 V since the load current was high and the ultracapacitor terminal voltage dropped. As described before, the power converter output current was controlled to equal the average current of the pulse load; therefore, the power converter worked in CCM during the entire load cycle no matter the load demand is high or low.

IV. Discussion

The performance of the active hybrid (shown in Fig. 3), comparing to the passive hybrid (shown in Fig. 1), is analyzed here in terms of their power capacity, discharge cycle time,

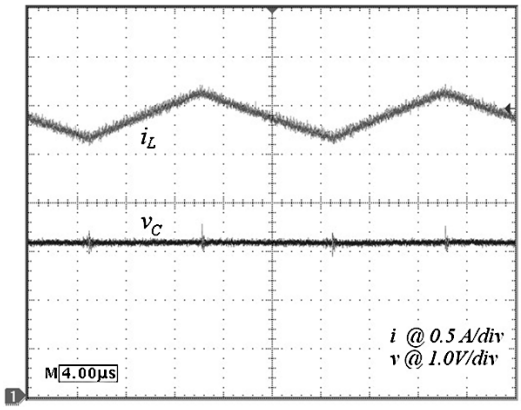

Fig. 13. Inductor current (0.5 A/div) and the converter output voltage (1 V/div) when the load demand is high.

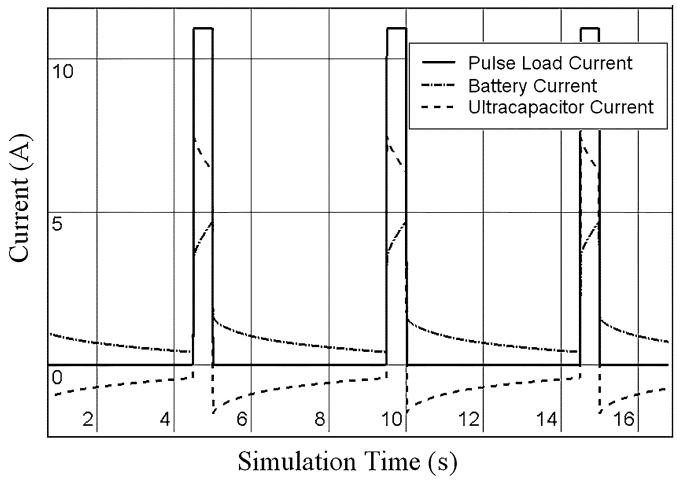

Fig. 14. Simulation results of the current waveforms of the passive hybrid.

specific power, and energy efficiency. It has been demonstrated previously that the virtual prototypes of the hybrid systems established in the VTB accurately represent the actual systems. Therefore, we will proceed with our analysis mostly based on the convenient simulation results; however, some of experimental results will also be furnished whenever it is necessary.

A. Power Capacity

Simulation studies of the passive battery/ultracapacitor hybrid were first conducted in the VTB to study its performance, as shown in Fig. 1. Notice that, to ensure that the ultracapacitor voltage did not exceed its rated value, the battery and ultracapacitor arrays were configured as follows: Two cells of batteries were connected in parallel, and two cells of ultracapacitors were connected in series. Simulation results are shown in Fig. 14. The battery supplied power to the load during the current pulse and to the ultracapacitor when the load current was zero. The ultracapacitor current was bi-directional and provided most of the current required by the load during the high current phase. The passive hybrid is able to supply a peak current value up to 11 A, and a peak power of 41.8 W (11×3.8), which is 2.3 times greater than that the battery alone (2×2.4 A $\times$ 3.8 V $=$18.24 W) can supply. Although the variation of battery current was reduced by using the ultracapacitor in parallel, there were still large variations that reached a peak value of 4.8 A at the end of each pulse

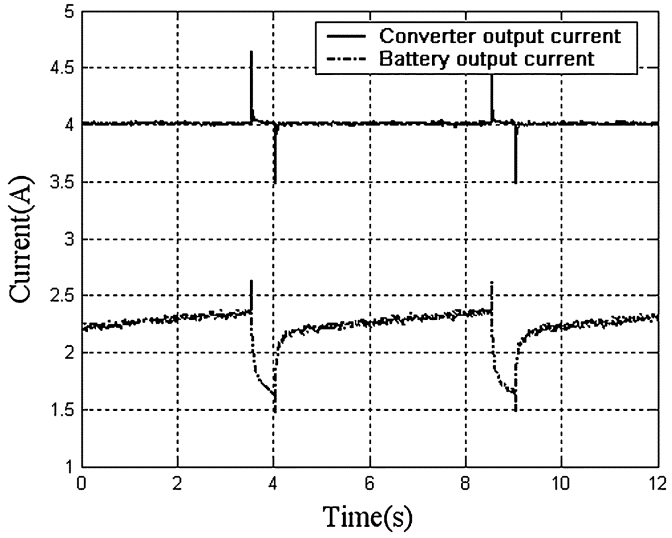

Fig. 15. Experimental results of the current waveforms of the active hybrid.

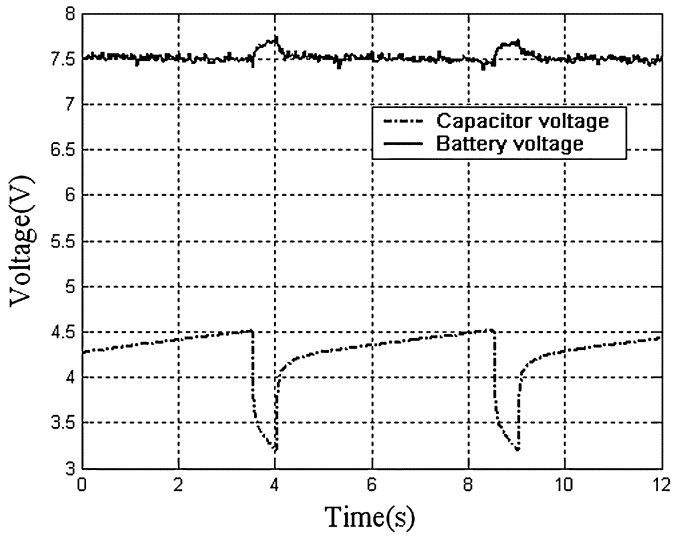

Fig. 16. Experimental results of the voltage waveforms of the active hybrid.

to a minimum value of 0.3 A at the beginning of each pulse. The power capacity of the hybrid source could be further improved by adding more ultracapacitors in parallel, but that will increase system volume, weight, and cost.

On the other hand, the configuration of the active hybrid allows the load voltage to be different from the battery voltage (7.5 V), which yields a battery cell current well below the safe limit while still satisfying the load power (41.8 W). For the constructed active hybrid, the maximum power capacity for the active system was experimentally determined by operating the battery at its safe limit, 2.4 A. By adjusting the load current to 40 A, the measured battery current became 2.38 A, nearly reaching the limit. This load current, together with a measured load voltage of 3.3 V, yielded a high power capacity of 132 W. The 40 A output current from the hybrid is approximately 14 times the battery C/1 rate, three times that of the passive system, and more than seven times that of the battery alone. Fig. 15 shows the battery and converter current waveforms obtained from the experiment. Notice that the battery current had a variation of about 0.7 A (2.38 A–1.68 A). Fig. 16 shows the battery and ultracapacitor voltage waveforms. The battery voltage was almost constant at about 7.5 V. The ultracapacitor voltage varied by about 1.31 V (4.51 V–3.2 V).

B. Discharge Cycle Time

The discharge cycle time is the time that the battery continuously discharges from the fully-charged state (100% SOC) to the discharged state at a cut-off voltage of 2.5 V for a given load profile. For both the active and passive hybrid systems, a pulse power load profile with a rate of 0.2 Hz, a duty ratio of 10%, a high power of 41.8 W, and a low power of 0 W was used. Note that this compares the performance of the active hybrid to that of the passive hybrid within a power range accessible to the passive hybrid. The power level is equivalent to that of the pulse current load profile in the previous simulation for the passive hybrid at a battery nominal voltage of 3.8 V.

Figs. 17 and 18 show the battery voltages in the passive and active hybrids respectively as a function of the simulation time for a complete discharge cycle. It can be seen that the cycle time

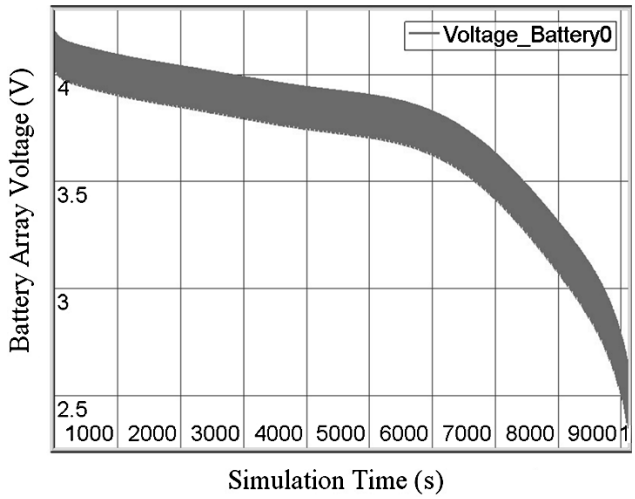

Fig. 17. Simulation result of the battery voltage of the passive hybrid.

for the passive system, 8969 seconds or 149.48 min, was longer than that of the active one, 8105 s or 135.08 min. The 14.4 min of cycle life reduction for the active system resulted from the added converter loss and the increased loss from the ultracapacitor since the ultracapacitor was operated at a high current level. This indicates that higher power capacity is at the cost of energy loss. Clearly, depending upon applications, optimized results can be achieved by making appropriate trade-offs between the power capability and the discharge cycle time. Also, the performance of the hybrid may be improved by simply incorporating those advances in power converter design that yield higher efficiencies. In Table II, some of the major power and energy parameters are listed for the two systems operated under the prescribed pulse power load profile.

Although the total loss was increased for the active system, the battery internal loss was actually reduced due to a very low constant current. In addition, the battery voltage ripples for the active system were much smaller compared to the ripple amplitude of 0.4 V for the passive system, as seen from Figs. 17 and 18. All of these contributed to a very stable and low temperature operation of the battery, which benefited the life of the battery.

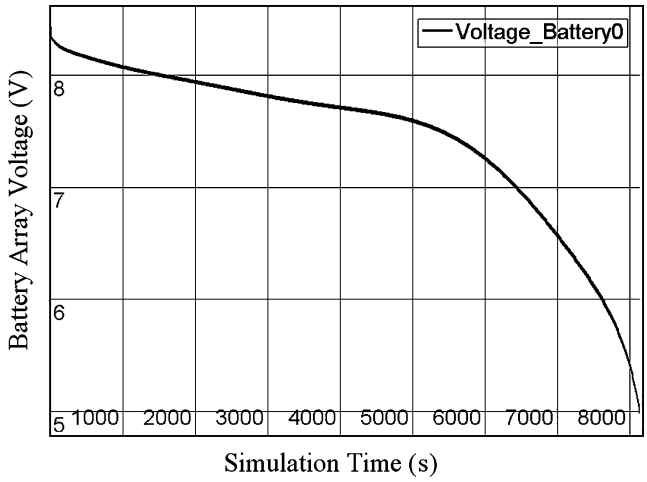

Fig. 18. Simulation result of the battery voltage of the active hybrid.

TABLE II
COMPARISON OF THE ENERGY DISTRIBUTION BETWEEN THE PASSIVE HYBRID AND THE ACTIVE HYBRID

	Passive Hybrid	Active Hybrid
Discharge Cycle Time (s)	8969	8105
Battery Delivered Energy (kJ)	38.11	38.69
Heat Generation in Battery (kJ)	3.63	2.07
Battery Final Temperature (K)	311	305
Energy Loss in Ultracapacitor (kJ)	0.62	1.97
Energy Received by Load (kJ)	37.49	33.87
Energy Loss in Converter (kJ)	n/a	2.85
Power Source Efficiency	89.8%	83.1%

Figs. 19 and 20 illustrate the battery surface temperatures as a function of the simulation time for the passive and active systems, respectively. In both cases, the battery surface was set up for a heat transfer coefficient of 4 W/m^2 K. As can be seen, the final temperature of the active system was 6-K lower than that of the passive hybrid.

C. Specific Power

Even though the converter contributes an increase in mass and volume, the specific power and power density are still dramatically increased for the active system due to its high power capacity. This is summarized in Table III in comparison to the passive and the battery-alone systems for the previously specified pulse current load condition (a period of 5 s and a duty ratio of 10%). It can be seen that the specific power of the active hybrid is 3.2 times that of the battery alone and 2.7 times that of the passive hybrid. The power density comparison yields similar results. The specific power and the power density are calculated based on the parameters of major power components only, and the system packaging and some auxiliary components are not considered here. It is clear that the active system is superior in terms of specific power and power density.

D. Energy Loss

Comparison of energy losses for the active and passive hybrids as well as for their components is shown in Fig. 21. Since the two systems have different power capabilities, as discussed in Part A of this section, the comparison must be made on the normalized basis, for which the loss is given here in terms of the energy loss in joules per joule of energy delivered as a function

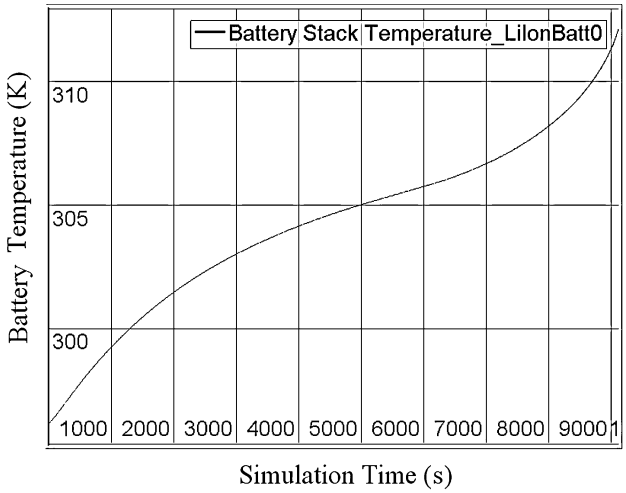

Fig. 19. Simulation result of the battery surface temperature of the passive hybrid.

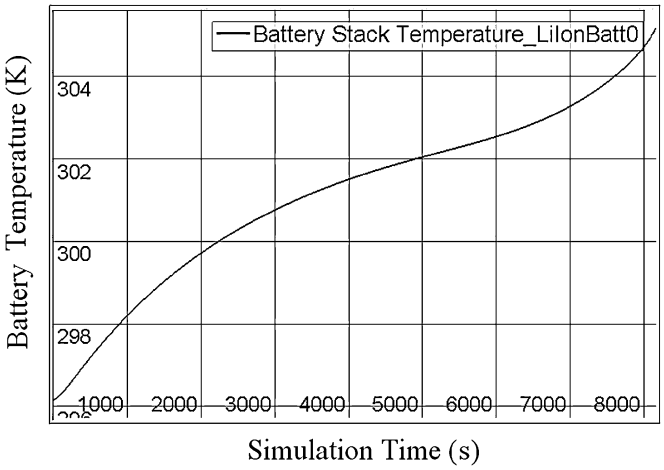

Fig. 20. Simulation result of the battery surface temperature of the active hybrid.

TABLE III
COMPARISON OF THE POWER CAPABILITY AMONG THREE KINDS OF POWER SOURCE UNDER SPECIFIED TEST CONDITION

	Battery Alone	Passive Hybrid	Active Hybrid
Configuration	2 cells in parallel	Battery: 2 cells in parallel Ultracapacitor: 2 cells in parallel	Battery: 2 cells in series Ultracapacitor: 2 cells in series
Weight (g)	84	158	188
Volume (cm^3)	138	202	232
Power capacity (W)	18.2	41.8	132
Specific power (W/kg)	217	264	702
Power density (W/cm^3)	0.132	0.207	0.570
Load voltage variation	1.7 V	1.7 V	< 1.31 V

of the duty ratio of the pulsed load power. It can be seen that, as the duty ratio increases, the energy loss in both the active and the passive hybrid power sources decreases since the operating current decreases. The active hybrid yields more total energy loss than the passive one because of two reasons: 1) added converter loss and 2) increased loss of ultracapacitor due to high current operation. The converter loss in fact amounts to about 50% of the total loss in the active system. However, the battery loss is reduced in the active system compared to that in the passive one. Also notice that the battery loss and the converter loss in the active system remain nearly constant as a result of battery constant

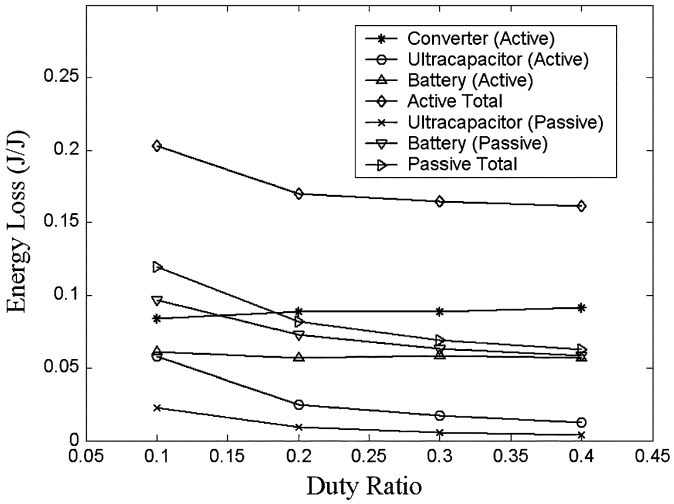

Fig. 21. Energy loss comparison between the passive hybrid and the active hybrid.

current operation. As indicated by this analysis, although the active hybrid has higher power capabilities, its energy efficiency is lower that that of the passive system. The comparison is given for the duty ratio ranging from 0.1 to 0.4. For higher duty ratios, the loss for a component or a system approaches a constant since the current approaches dc operation; this is beyond the scope of this paper.

Finally, we would like to point out that, although the performance evaluation is given for some specific power profiles, the results are scalable for different power levels as long as the load power is pulsed.

V. Conclusion

The simulation and experimental studies of an active hybrid battery/ultracapacitor power source have been presented in terms of power enhancement, discharge cycle life, specific power, and energy loss with respect to pulse load profiles. It has been shown that the active hybrid yields a peak power 3.2 times that of a passive hybrid, and a specific power 2.7 times that of a passive hybrid. Furthermore, the operation of an active hybrid results in a much lower battery current with very small ripples, and therefore a lower battery temperature, which are preferred by many applications for a longer battery lifetime. The discharge cycle time is reduced for the active hybrid due to an added converter loss and increased ultracapacitor loss. A compromise should be made between the power enhancement and the discharge cycle time in order to achieve optimized results depending upon applications. The design can be scaled to larger or smaller power capacities for various applications.

References

[1] A. Yoshida, K. Imoto, H. Yodeda, and A. Nishino, "An electric double-layer capacitor with high capacitance and low resistance," *IEEE Trans. Compon., Hybrids, Manufact. Technol.*, vol. 15, no. 1, pp. 133–138, Feb. 1992.

[2] B. E. Conway, *Electrochemical Supercapacitors: Scientific Fundamentals and Technological Applications*. New York: Plenum, 1999.

[3] H. L. Lee, G. L. Bullard, G. E. Mason, and K. Kern, "Improved pulse power sources with high-energy density capacitor," *IEEE Trans. Magn.*, vol. 25, no. 1, pp. 324–330, Jan. 1989.

[4] J. R. Miller, "Battery-capacitor power source for digital communication applications: Simulations using advanced electrochemical capacitors," in *Proc. Electrochemical Soc.*, vol. 95-29, Oct. 1995, pp. 246–254.

[5] J. P. Zheng, T. R. Jow, and M. S. Ding, "Hybrid power sources for pulsed current applications," *IEEE Trans. Aerosp. Electron. Syst.*, vol. 1, no. 1, pp. 288–292, Jan. 2001.

[6] R. A. Dougal, S. Liu, and R. E. White, "Power and life extension of battery-ultracapacitor hybrids," *IEEE Trans. Compon. Packag. Technol.*, vol. 25, no. 1, pp. 120–131, Mar. 2002.

[7] H. W. Brandhorst Jr. and Z. Chen, "Achieving a high pulse power system through engineering the battery-capacitor combination," in *Proc. 16th Annu. Battery Conf. Applications Advances*, Jan. 2001, pp. 153–156.

[8] R. A. Dougal, C. W. Brice, R. O. Pettus, G. Cokkinides, and A. P. S. Meliopoulos, "Virtual prototyping of PCIM systems—The virtual test bed," in *Proc. PCIM/HFPC'98 Conf.*, Santa Clara, CA, Nov. 1998, pp. 226–234.

[9] R. Dougal, S. Liu, L. Gao, and M. Blackwelder, "Virtual test bed for advanced power sources," *J. Power Sources*, vol. 110, no. 2, pp. 285–294, Aug. 2002.

[10] *Electronics Engineers' Handbook*, 3rd ed., D. G. Fink and D. Christiansen, Eds., McGraw-Hill, New York, 1989.

[11] L. Gao, S. Liu, and R. A. Dougal, "Dynamic lithium-ion battery model for system simulation," *IEEE Trans. Compon. Packag. Technol.*, vol. 25, no. 3, pp. 495–505, Sep. 2002.

[12] R. A. Dougal, L. Gao, and S. Liu, "Ultracapacitor model with automatic order selection and capacity scaling for dynamic system simulation," *J. Power Sources*, vol. 126, pp. 250–257, Feb. 2004.

[13] Solutions for control (2004, May). [Online]. Available: http://www.dspaceinc.com/ww/en/inc/home.htm

Lijun Gao (M'04) received the Ph.D. degree in electrical engineering from the University of South Carolina, Columbia, in 2003.

His current research interests include design and control of advance hybrid power sources and systems, modeling and simulation of hybrid electric vehicles (HEVs), artificial intellgience based applications in electrochemical energy components, and advanced motor control.

Roger A. Dougal (S'74–M'78–SM'94) received the Ph.D. degree in electrical engineering from Texas Tech. University, Lubbock, in 1983.

He then joined the faculty at the University of South Carolina, Columbia. He is the Director of the Virtual Test Bed Project, which is developing an advanced simulation and virtual prototyping environment for multidisciplinary dynamic systems.

Dr. Dougal received the Samuel Litman Distinguished Professor of Engineering Award.

Shengyi Liu (S'94–M'96–SM'03) received the Ph.D. degree in electrical engineering from the University of South Carolina (USC), Columbia, in 1995.

He was a Senior Research and Development Engineer at InnerLogic, Inc., from 1995 to 1999, and is now a Research Associate Professor in the Department of Electrical Engineering, USC. Research interests include design and development of energy storage technologies, physical electronics-based devices, power semiconductor devices and converters, application and control of advanced power sources, renewables, autonomous power systems, and modeling and simulation of interdisciplinary systems.